UC Santa Barbara

UC Santa Barbara Previously Published Works

Title

Heterogeneous integration of a III-V quantum dot laser on high thermal conductivity silicon carbide.

Permalink

https://escholarship.org/uc/item/2xb5h14p

Journal

Optics letters, 48(10)

ISSN

0146-9592

Authors

Koscica, Rosalyn
Wan, Yating
He, William
et al.

Publication Date

2023-05-01

DOI

10.1364/ol.486089

Copyright Information

This work is made available under the terms of a Creative Commons Attribution License, availalbe at https://creativecommons.org/licenses/by/4.0/

Peer reviewed

eScholarship.org Powered by the California Digital Library
University of California

OPTICA PUBLISHING GROUP | Formerly OSA
LOGIN | CREATE ACCOUNT | PRISM SUBMISSION
JOURNALS CONFERENCES PREPRINTS OTHER RESOURCES MY FAVORITES RECENT PAGES
JOURNAL HOME ABOUT ISSUES IN PROGRESS CURRENT ISSUE ALL ISSUES EARLY POSTING

Optics Letters Vol. 48, Issue 10, pp. 2539-2542 (2023) • https://doi.org/10.1364/OL.486089

Heterogeneous integration of a III–V quantum dot laser on high thermal conductivity silicon carbide

Rosalyn Koscica, Yating Wan, William He, M. J. Kennedy, and John E. Bowers
Author Information ▾ Find other works by these authors ▾

Accessible
Full-text access provided by University of California Santa Barbara (CDL)
Get PDF Email Share Get Citation Citation alert Save article
PDF Article
Article Outline
Figures (2)
Data Availability
References (30)
Cited By (0)
Back to Top

Abstract

Heat accumulation prevents semiconductor lasers from operating at their full potential. This can be addressed through heterogeneous integration of a III–V laser stack onto non-native substrate materials with high thermal conductivity. Here, we demonstrate III–V quantum dot lasers heterogeneously integrated on silicon carbide (SiC) substrates with high temperature stability. A large T_0 of 221 K with a relatively temperature-insensitive operation occurs near room temperature, while lasing is sustained up to 105°C. The SiC platform presents a unique and ideal candidate for realizing monolithic integration of optoelectronics, quantum, and nonlinear photonics.

© 2023 Optica Publishing Group

Introduction. Heterogeneous integration of III–V epitaxial material with non-native substrates has the potential to create equally or better performing devices than those previously demonstrated using only III–V materials. In recent years, commercialization prospects have promoted heterogeneous integration on silicon and silicon-on-insulator (SOI) wafers, owing to the low-cost and scalable manufacturing potential of CMOS-compatible platforms [1]. However, other potential non-native substrate materials with beneficial thermal or optical properties remain as yet less explored.

The III–V quantum dot (QD) laser is a particularly interesting candidate for heterogeneous integration, owing to its inherent structural advantages over quantum well (QW) counterparts, including superior defect tolerance and thermal stability of optical gain [2–4]. In addition to the superior performance seen in simple Fabry–Pérot cavity lasers, the QD active region enables development of complex photonic light sources, such as microring lasers [5], distributed feedback (DFB) lasers [6–8], coupled cavity tunable lasers [9], and photonic crystal lasers [10].

QD lasers as-grown on native substrate are limited by the thermal properties and fabrication constraints of a III–V platform, such as lower processing temperatures and incompatibility with silicon-based passive components. Despite tremendous progress in heteroepitaxial growth technique, ongoing efforts in direct monolithic growth of III–V material on silicon substrate have yet to match the performance of native-grown devices [3,4,11]. By contrast, heterogeneous integration methods enable placement of fully functional, high-performance native-grown QD lasers on a non-native substrate compatible with other critical photonic components. Recently, heterogeneous methods produced record high-speed DFB QD lasers bonded to silicon substrate [7,8]. This successful transfer of QD lasers indicates a corresponding refinement of the fabrication methods for heterogeneously integrated photonic devices. A natural next step is to bring QD lasers to additional non-native platforms, with the potential to enhance device and chip-scale performance.

The push toward integrated photonic technologies drives an increasing demand for high-power light sources that can be densely packed within a small volume. In particular, datacenter interconnects for telecommunications require co-packaged optics and electronics in close proximity. These combined devices can generate considerable heat during operation; for instance, a single application-specific integrated circuit (ASIC) switch can consume over 200 W power [12]. Increased thermal load within a laser chip with high device density alters optical output, diminishes performance, and degrades overall device lifetime. This creates a trade-off between high packing density and effective laser performance, which in turn poses considerable difficulty when adapting photonic light sources to applications with limited physical space.

Heat accumulation can be mitigated by using the substrate as a heatsink, but the effectiveness of this method depends on the thermal conductivity of the substrate material. Compared with native GaAs substrate with a thermal conductivity of 0.55 W/cm·K at 300 K [13] and undoped silicon with a higher thermal conductivity of 1.3 W/cm·K at 300 K [14], SiC possesses an impressively high thermal conductivity of 4.9 W/cm·K at 300 K [15]. In addition, SiC has high breakdown voltage (3×10^6 V/cm) [16], high optical damage threshold (80 GW/cm^2) [17], and nonlinear effects at the second order (30 pm/V) and third order (10^{-18} m^2/W) [18,19], which make the SiC platform a unique and ideal candidate for multi-component integration.

Pioneering work proposed the III–V on SiC photonics platform, where InP and InGaAsP waveguides were successfully transferred to bulk SiC substrate [20]. Further characterization of III–V bonded to SiC revealed heat dissipation improvement by a factor of nine, as well as reduced thermal stress of InP films on SiC, compared with silicon or SOI substrates [21]. While properties of III–V lasers on heterogeneously bonded silicon platforms have been extensively studied [1,22,23], there has been limited research regarding III–V lasers integrated on SiC substrates. Recent studies in membrane device processing show promising high-speed performance of membrane lasers on SiC substrate operated under direct modulation [24]. Preliminary work also shows that the SiC platform enables production of photonic crystals [25], nonlinear microresonators [19], and long-coherence spin-defect based photonics for quantum computing [19,26]. Moving forward, comprehensive research in the work flow to heterogeneously integrate III–V lasers onto SiC is needed.

In this study, we use chip-scale heterogeneous integration to bond InAs QD lasers onto high thermal conductivity SiC substrate. These Fabry–Pérot lasers emit in the O-band at room temperature and sustain lasing up to 105°C, with a relatively temperature-insensitive characteristic temperature T_0 of 221 K. Additionally, these devices begin to lase with threshold current density as low as 223 A/cm^2. Although this first demonstration of QD lasers on SiC still allows significant room for improvement in output power levels, this can be addressed in future iterations with modification of the optical mode profile and QD active region. The low-threshold current density and temperature-insensitive performance of these lasers indicates high potential for the use of thermally conductive SiC in further laser applications.

Molecular beam epitaxy (MBE) is used to grow a III–V laser structure on a native (001) GaAs substrate. This structure targets the center of the gain spectrum within the O-band at 1300 nm wavelength. Figure 1 shows, schematically, the epitaxial structure as-grown. The (001) GaAs substrate is coated with 500 nm $Al_{0.8}Ga_{0.2}As$ that will be removed after bonding. The device stack has the following structure, from top to bottom: 400 nm p-GaAs p-contact, 50 nm p-$Al_xGa_{(1-x)}As$ graded from $x = 0$ to 0.4, 1.4 µm p-$Al_{0.4}Ga_{0.6}As$ p-cladding, 20 nm p-$Al_xGa_{(1-x)}As$ graded from $x = 0.4$ to 0.2, 30 nm p-$Al_{0.2}Ga_{0.8}As$ separate confinement heterostructure (SCH), five repeats of InAs QD in InGaAs QW gain medium with p-modulation doped GaAs spacers at a doping level of 10 holes per QD, 30 nm n-$Al_{0.2}Ga_{0.8}As$ SCH, 150 nm n-GaAs n-cladding, and a strained-layer superlattice (SLS) of alternating 10 nm each n-$Al_{0.3}Ga_{0.7}As$/n-GaAs. The SLS compensates for stress from the lattice mismatch between III–V and the SiC substrate after bonding.

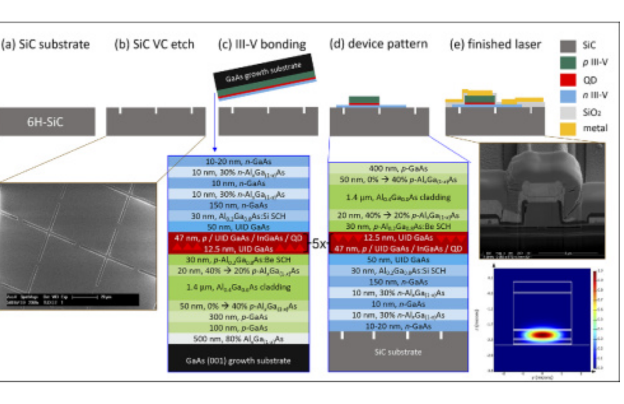

Fig. 1. Processing steps from bonded wafer to complete device. (a) SiC substrate. (b) Substrate is etched to create vertical channels (VCs) before bonding. A top view is imaged using scanning electron microscopy. (c) III–V laser stack epitaxially grown on native GaAs is bonded to SiC substrate. (d) Device mesas are defined and etched, resulting in the laser material structure. (e) Cross sectional schematic, scanning electron micrograph of completed laser, and simulated normalized intensity profile of optical mode.
Download Full Size | PDF

The initial substrate is a commercially available, semi-insulating 2 in. 6H-SiC (0001) wafer doped with vanadium to a vendor-specified resistivity over 10^5 Ω·cm. The fresh SiC wafer is prepared for bonding by dry etching a grid-shaped pattern of vertical channels (VCs) across the top surface with 50 µm pitch in both directions, as shown schematically and imaged in Figs. 1(a) and 1(b), respectively. This dry etching is done through inductively coupled plasma (ICP) reactive ion etching (RIE) with SF_6 gas. Directly before bonding, the as-grown III–V material and VC-patterned SiC wafer surfaces are prepared with N-methyl-2-pyrrolidone (NMP) solution, followed by oxygen plasma ashing and piranha acid cleaning. The III–V laser stack as-grown on native GaAs is flip-chip bonded onto the SiC wafer with a 3 nm SiO_2 interlayer, and the structure is subsequently annealed at 100°C for 18–24 h to relieve residual stress after bonding [Fig. 1(c)]. After returning to room temperature, the coefficient of thermal expansion difference between the substrate and the bonded film results in a tensile strained III–V stack. The VC pattern in the SiC/III–V interface allows any trapped gases from this bonding step to escape during subsequent processing stages. After bonding, the GaAs growth wafer and AlGaAs buffer are polished away during the substrate removal step.

The initial laser profiles are patterned using photolithography and a two-step Cl_2/N_2 dry etch. The first dry etch defines the p-mesa and laser facets, while the second etch creates the wider n-mesa [Fig. 1(d)]. Pd/Ge/Au/Ti contact metal is deposited along the n-mesa. The structure is passivated with sputtered SiO_2. Another dry etch using CHF_3/CF_4 opens vias in the SiO_2 covering the n-mesa and p-mesa. Pd/Ti/Au/Pd/Ti contact metal is then deposited on the p-mesa, followed by a rapid thermal anneal (RTA) in forming gas for 60 s at 300°C and plasma-enhanced chemical vapor deposition (PECVD) of a second SiO_2 passivation layer. Finally, the n-contact and p-contact vias are dry-etched in CHF_3/CF_4 to open the second passivation layer, and up to 1.5 µm additional Ti/Au probe metal is deposited across the device for electrical injection during characterization [Fig. 1(e)]. This follows the optimized fabrication methods used to develop our previous heterogeneous lasers on silicon [7]. Throughout fabrication, the sample temperature is limited to a maximum of 300°C to reduce the risk of thermally induced strain or cracking on the bonded material. After completion of all fabrication steps, the chip is diced and polished into bars of Fabry–Pérot lasers. The full series of devices include dimensions of length 1500 µm to 2500 µm and p-mesa width ranging from 1.5 µm to 3 µm. The electric field intensity profile of the optical mode for a 3 µm mesa device is shown in Fig. 1(e).

Results. The heterogeneous QD III–V on SiC lasers are measured on a temperature-controlled stage under continuous wave (CW) electrical injection. Both laser facets are dry-etched surfaces with no additional coating applied. An integrating sphere collects optical device output during light–current–voltage (LIV) measurements. Spectrum measurements are made with the device output coupled through a lens fiber to an optical spectrum analyzer (OSA).

[illegible]

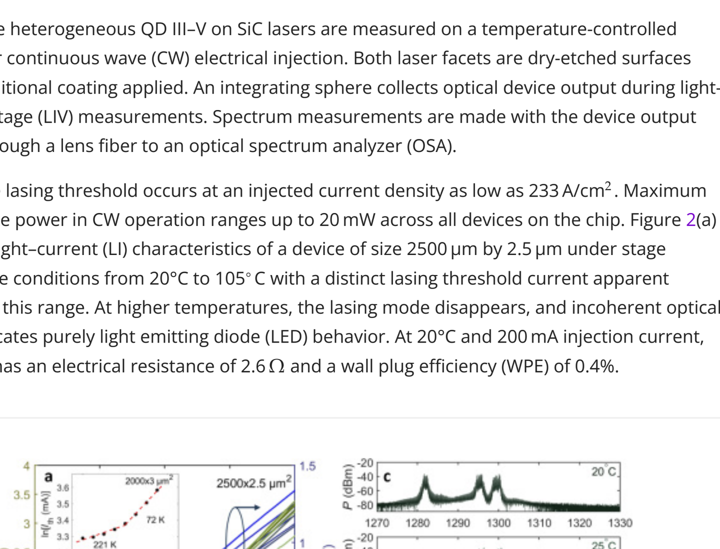

Fig. 2. [illegible]

[illegible] silicon-substrate lasers shows the progress slope inherent to any new platform, suggesting potential for improvement in SiC laser performance with further study.

Lasing peaks occur between 1290 nm and 1305 nm during standard 20°C operation. The ground state is typically centered at 1300 nm with the first excited state emerging at 1295 nm. Spectra taken at varying temperatures and a fixed injection current of 100 mA indicate a thermal redshift of 0.106 nm/°C when tracking the same peak across temperatures. Spectra taken at a fixed temperature of 20°C and varying injection current indicate a current-driven redshift of 5.64 nm/A when tracking the same peak across currents [Fig. 2(b)].

At injection currents beyond threshold, the emission spectra of these devices show two or more distinct peaks. In Fig. 2(c), changing the temperature from 20°C to 45°C at a constant injection current of 100 mA generates between two and four peaks. It is unclear why the spectra show a number of sparse peaks, given the Fabry–Pérot device design, but this might indicate unintentional internal reflection from the optical defects that interfere with the laser cavity or facet mirrors. The facets of these III–V on SiC devices appear intact when imaged, as seen in Fig. 1(e). Nevertheless, the multi-peak spectra might indicate a need for further process refinement to optimize device geometry and reflectivity.

Conclusion. SiC substrate is an ideal candidate for heterogeneous integration of QD lasers, owing to its high inherent thermal conductivity, as well as the prevalence of nonlinear and quantum computing technologies already established on the SiC platform. In this study, we show that InAs/GaAs QD lasers can be successfully transferred to SiC substrate through flip-chip bonding. The SiC-bonded lasers achieve a low lasing threshold current density of 233 A/cm^2 and promising thermal characteristics. A high T_0 of 221 K indicates a thermally insensitive operation regime near room temperature, and laser operation is sustained up to 105°C environmental temperature. This Fabry–Pérot laser demonstration presents a preliminary success in III–V light source integration on a SiC platform.

Further work developing the bonding process and testing device reliability will be essential to achieve performance comparable with state-of-the-art heterogeneous integration of III–V on silicon substrate. With an optimized bonding procedure, the SiC platform will enable integration of III–V light sources with more technology-specific applications, such as DFB or comb lasers for telecommunications. This study's successful demonstration of bonded QD lasers on the SiC platform represents a first step toward that eventuality, setting the foundation for future integrated photonic technologies that enhance on-chip light source performance using SiC material properties.

Beyond leveraging the improved thermal conductivity of the SiC platform, further extensions include combining these QD lasers with the nonlinear resonators and quantum computing technologies unique to the SiC platform. For instance, DFB lasers could enable direct on-chip control over spin-defect qubits in SiC. Overall, adding heterogeneous III–V components to existing quantum computing systems merges the advantages of devices optimized for each platform. This, in turn, promotes the development of photonic circuits where all necessary components coexist within a single chip.

Acknowledgments

A portion of this work was performed in the UCSB Nanofabrication Facility. We thank Lin Chang for providing the SiC substrates and Mario Dumont for helpful discussion.

Disclosures

The authors declare no conflicts of interest.

Data availability

Data underlying the results presented in this paper are not publicly available at this time but may be obtained from the authors upon reasonable request.

REFERENCES

1. C. Xiang, W. Jin, D. Huang, M. A. Tran, J. Guo, Y. Wan, W. Xie, G. Kurczveil, A. M. Netherton, D. Liang, H. Rong, and J. E. Bowers, IEEE J. Sel. Top. Quantum Electron. **28**, 8200515 (2022). [CrossRef]

2. Y. Arakawa and H. Sakaki, Appl. Phys. Lett. **40**, 939 (1982). [CrossRef]

3. J. Norman, D. Jung, Z. Zhang, Y. Wan, S. Liu, C. Shang, R. Herrick, W. Chow, A. Gossard, and J. Bowers, IEEE J. Quantum Electron. **55**, 2000511 (2019). [CrossRef]

4. C. Shang, Y. Wan, J. Selvidge, E. Hughes, R. Herrick, K. Mukherjee, J. Duan, F. Grillot, W. Chow, and J. Bowers, ACS Photonics **8**, 2555 (2021). [CrossRef]

5. Y. Wan, J. Norman, Q. Li, M. J. Kennedy, D. Liang, C. Zhang, D. Huang, Z. Zhang, A. Y. Liu, A. Torres, D. Jung, A. C. Gossard, E. L. Hu, K. M. Lau, and J. E. Bowers, Optica **4**, 940 (2017). [CrossRef]

6. Y. Wang, S. Chen, Y. Yu, L. Zhou, L. Liu, C. Yang, M. Liao, M. Tang, Z. Liu, J. Wu, W. Li, I. Ross, A. J. Seeds, H. Liu, and S. Yu, Optica **5**, 528 (2018). [CrossRef]

7. Y. Wan, C. Xiang, J. Guo, R. Koscica, M. Kennedy, J. Selvidge, Z. Zhang, L. Chang, W. Xie, D. Huang, A. Gossard, and J. Bowers, Laser Photonics Rev. **15**, 2100057 (2021). [CrossRef]

8. D. Liang, S. Srinivasan, A. Descos, C. Zhang, G. Kurczveil, Z. Huang, and R. Beausoleil, Optica **8**, 591 (2021). [CrossRef]

9. Y. Wan, S. Zhang, J. C. Norman, M. J. Kennedy, W. He, S. Liu, C. Xiang, C. Shang, J.-J. He, A. C. Gossard, and J. E. Bowers, Optica **6**, 1394 (2019). [CrossRef]

10. T. Zhou, M. Tang, G. Xiang, B. Xiang, S. Hark, M. Martin, T. Baron, S. Pan, J.-S. Park, Z. Liu, S. Chen, Z. Zhang, and H. Liu, Nat. Commun. **11**, 977 (2020). [CrossRef]

11. J.-S. Park, M. Tang, S. Chen, and H. Liu, *Semiconductor Nanodevices* (Elsevier, 2021), pp. 353–388.

12. M. Bohn, P. Magill, M. Hochberg, D. Scordo, A. Novack, and M. Streshinsky, in *2019 Optical Fiber Communications Conference and Exhibition (OFC)* (2019), pp. 1–3.

13. R. O. Carlson, G. A. Slack, and S. J. Silverman, J. Appl. Phys. **36**, 505 (1965). [CrossRef]

14. C. J. Glassbrenner and G. A. Slack, Phys. Rev. **134**, A1058 (1964). [CrossRef]

15. G. A. Slack, J. Appl. Phys. **35**, 3460 (1964). [CrossRef]

16. Y. Goldberg, M. Levinshtein, and S. Rumyantsev, *Properties of Advanced Semiconductor Materials : GaN, AlN, InN, BN, SiC, SiGe* (John Wiley & Sons, 2001).

17. M. Naftaly, J. Molloy, B. Magnusson, Y. Andreev, and G. Lanskii, Opt. Express **24**, 2590 (2016). [CrossRef]

18. R. Adair, L. L. Chase, and S. A. Payne, Phys. Rev. B **39**, 3337 (1989). [CrossRef]

19. C. Wang, Z. Fang, A. Yi, B. Yang, Z. Wang, L. Zhou, C. Shen, Y. Zhu, Y. Zhou, R. Bao, L. Xu, Y. Chen, K. Huang, J. Zhang, Y. Cheng, and X. Ou, Light: Sci. Appl. **10**, 139 (2021). [CrossRef]

20. M. Takenaka and S. Takagi, Opt. Express **25**, 29993 (2017). [CrossRef]

21. T. Sanjoh, N. Sekine, K. Kato, S. Takagi, and M. Takenaka, Jpn. J. Appl. Phys. **58**, SBBE06 (2019). [CrossRef]

22. S. Fathpour, Nanophotonics **4**, 143 (2015). [CrossRef]

23. G.-H. Duan, S. Olivier, S. Malhouitre, A. Accard, P. Kaspar, G. de Valicourt, G. Levaufre, N. Girard, A. L. Liepvre, A. Shen, D. Make, F. Lelarge, C. Jany, K. Ribaud, F. Mallecot, P. Charbonnier, H. Gariah, C. Kopp, and J.-L. Gentner, J. Lightwave Technol. **33**, 976 (2015). [CrossRef]

24. S. Yamaoka, P. Diamantopoulos, H. Nishi, R. Nakao, T. Fujii, K. Takeda, T. Hiraki, T. Tsurugaya, S. Kanazawa, H. Tanobe, T. Kakitsuka, T. Tsuchizawa, F. Koyama, and S. Matsuo, Nat. Photonics **15**, 28 (2021). [CrossRef]

25. S. Yamada, B.-S. Song, T. Asano, and S. Noda, Appl. Phys. Lett. **99**, 201102 (2011). [CrossRef]

26. D. M. Lukin, M. A. Guidry, and J. Vučković, PRX Quantum **1**, 020102 (2020). [CrossRef]

27. QD Laser Inc., "Semiconductor lasers / epitaxial wavers," 2023, https://www.qdlaser.com/en/products/list.html.

28. T. Kageyama, K. Nishi, M. Yamaguchi, R. Mochida, Y. Maeda, K. Takemasa, Y. Tanaka, T. Yamamoto, M. Sugawara, and Y. Arakawa, in *2011 Conference on Lasers and Electro-Optics Europe and 12th European Quantum Electronics Conference (CLEO EUROPE/EQEC)* (2011), p. 1.

29. Y. Wan, C. Shang, J. Norman, B. Shi, Q. Li, N. Collins, M. Dumont, K. M. Lau, A. C. Gossard, and J. E. Bowers, IEEE J. Sel. Top. Quantum Electron. **26**, 1900409 (2020). [CrossRef]

30. C. Shang, E. Hughes, Y. Wan, M. Dumont, R. Koscica, J. Selvidge, R. Herrick, A. C. Gossard, K. Mukherjee, and J. E. Bowers, Optica **8**, 749 (2021). [CrossRef]